Tetrahedron 71 (2015) 2863–2871

Contents lists available at ScienceDirect

Tetrahedron

journal homepage: www.elsevier.com/locate/tet

Quantum chemical investigation of the origin of activation of S_N2 type halogenation by oligo-ethylene glycol—ionic liquids

Sung-Sik Lee [a,†], Vinod H. Jadhav [b,†], Ju-Young Kim [a], Ji-Hoon Chun [a], Aram Lee [a], Su-Yeon Kim [a], Sungyul Lee [a,*], Dong Wook Kim [b,*]

[a] Department of Applied Chemistry, Kyung Hee University 1732, Duckyoung-daero 1732, Gihung-gu, Yongin-si, Gyeonggi-do 446-701, South Korea
[b] Department of Chemistry, Inha University, 100 Inha-ro, Nam-gu, Incheon 402-751, South Korea

ARTICLE INFO

Article history:
Received 8 February 2015
Received in revised form 16 March 2015
Accepted 19 March 2015
Available online 26 March 2015

Keywords:
Multifunctional promotors
S_N2
Dihexa-ethylene glycol
Imidazolium salt
Alkali metal

ABSTRACT

We demonstrate the efficiency of dihexa-ethylene glycol (dihexaEG) substituted imidazolium salts (dihexaEGIms) as promoters for S_N2 reactions, which could significantly enhance the nucleophilicity of alkali metal salts by producing the 'naked' nucleophiles from the metal salts KX (X=F, Cl, Br). We demonstrate by quantum chemical calculations that this almost complete dissociation of metal salts is the results of the synergetic effects of the dihexaEG and the ionic liquid moieties. We also examine the role of solvent (*tert*-amyl alcohol), finding that the solvent molecule influences the reaction indirectly by interacting with the promotor rather than the metal salt. The calculated relative activation barriers for reactions of the nucleophiles F^-, Cl^- and Br^- are in excellent agreement with the experimentally observed relative reactivity of the halides $F^->Cl^->Br^-$.

© 2015 Elsevier Ltd. All rights reserved.

1. Introduction

Recent progress in bimolecular nucleophilic substitution (S_N2) reaction[1–18] has demonstrated that this fundamental and very useful type of chemical reaction must still be studied systematically, especially for the role of counter-cation and solvent[19–21] for their efficacy. Use of metal salts and protic solvents[22–34] (bulky alcohols and oligoethylene glycols) seems to have opened a breakthrough for this purpose. Careful mechanistic studies have suggested that the nucleophile reacts as an ion-pair, but the strongly retarding Coulombic influence of the counter-cation on the nucleophile is 'neutralized' by protic solvents acting as Lewis base. Promotion of S_N2 reactions by ionic liquids[34–42] was also understood to proceed by similar mechanism: The ionic liquid anion interacts with the counter-cation as Lewis base.[34] It was also demonstrated that crown ethers,[43–47] which have been instrumental for facilitating the S_N2 reactions, do *not* actually 'separate' the nucleophile from the counter-cation as envisaged for so long, but rather bind to the ion-pair metal salts.[42,47]

The role of ion-pair[48–52] versus naked nucleophile for S_N2 reactions is a very important issue. Although our previous works[22–34,42] demonstrated that metal halides as contact ion pair (CIP) may be very effective reagents for S_N2 reactions in the presence of Lewis base solvents, separation of the metal cation (Cs^+ and K^+) from the nueclophile may further enhance the rate constants of S_N2 reactions. So far, we have not seen any situation in which the solvents or the promoters give 'naked' nucleophile that is detached from the metal cation. It seems that much stronger Lewis base is necessary for this purpose, stronger than bulky alcohols, oligoethylene glycols, and the ionic liquid anions that were employed in our previous works.

Herein, we demonstrate that dihexa-ethylene glycol substituted imidazolium salts (dihexaEGILs) may indeed produce such a 'separated' metal salt ion pair, and that the enhanced reaction rates of S_N2 reactions by this promoter over those of monohexa-ethylene glycol substituted imidazolium salts are the results of this effect. The synergetic effects of the dihexaEG and the ionic liquid moieties seem to be the origin of this rate increase. We also examine the role of protic solvent (*tert*-amyl alcohol), showing that the solvent influences the reaction indirectly by interacting with the functional groups in the promotor rather than directly with the metal salt. Our quantum chemical calculations are in excellent agreement with the experimentally observed order of reactivity $F^->Cl^->Br^-$.

* Corresponding authors. Tel.: +82 31 201 2423; fax: +82 31 201 2340 (S.L.); tel.: +82 32 860 7679; fax: +82 32 867 5604 (D.W.K.); e-mail addresses: sylee@khu.ac.kr (S.-S. Lee), kimdw@inha.ac.kr (D.W. Kim).
† These authors contributed equally to this work.

http://dx.doi.org/10.1016/j.tet.2015.03.074
0040-4020/© 2015 Elsevier Ltd. All rights reserved.

2. Results and discussion

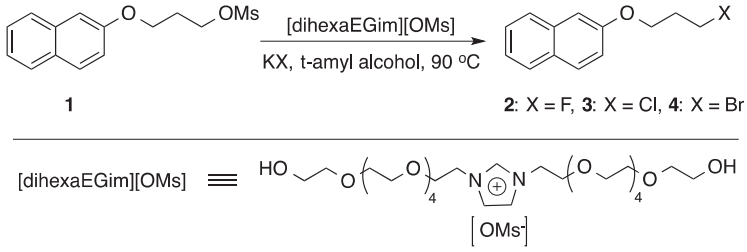
2.1. Promotion of S_N2 reactions by dihexaEGILs

In order to investigate the efficiency of 1,3-dihexaethylene glycolic imidazolium mesylate salt [dihexaEGim][OMs] as a promoter for various S_N2 halogenation reactions, we carried out the nucleophilic substitution (S_N2) reactions of 2-(3-methanesulfonyloxy propyl)naphthalene (**1**) using various potassium halides (KXs) such as KF, KCl and KBr in the presence of [dihexaEGim][OMs] in *tert*-amyl alcohol at 90 °C as shown in Scheme 1. The observed rates of S_N2 reactions are presented in Fig. 1. It is well-known that the generalized order of potassium halide reactivity is KBr>KCl>KF depending on their ionic strength between potassium cation and halide nucleophiles. In particular, The S_N2 reaction using KF in polar aprotic medium proceed hardly compared with other KXs. However, in the presence of [dihexaEGim][OMs] in the bulky protic solvent, the S_N2 reaction using KF was observed to show the fastest reaction rate, providing the corresponding fluoro-product **2** in 98% yield within 2 h. This certainly is a significant advance in S_N2 catalysis, because the observed rate increase is larger than that (~83% yield in 2 h) achieved by the promotor [monohexaEGim][OMs] in our previous work[42] using CsF in which Cs^+ of much larger polarizability (and thus, much smaller retarding Coulombic influence on the nucleophile) was employed. Moreover, the nucleophilic reaction using KCl also proceeded slightly faster than the reaction using KBr; consequently, in this reaction condition, the order of potassium halide reactivity was observed to be KF>KCl>KBr. These interesting observations on the relative rates of S_N2 fluorination, chlorination and bromination certainly require a systematic study of the mechanism for these reactions, particularly for the role of the promotor [dihexaEGim][OMs] and the *protic* solvent *tert*-amyl alcohol. Our findings seems to suggest that very intricate interactions between the counter-cation K^+, the nucleophile, the promotor, solvent molecules and the leaving group may give excellent reaction rates for S_N2 halogenation reactions, and the non-conventional relative S_N2 reactivities F^->Cl^->Br^-.

2.2. Mechanism of S_N2 reactions promoted by dihexaEGILs: ion-pair nucleophile versus naked nucleophile

We examined the mechanism of fluorination, chlorination and bromination reactions by obtaining the structures of pre-reaction complexes, transition states, and post-reaction complexes by quantum chemical methods[53,54] (MPW1K/6-31G*/LANL2DZ with effective core potential[55] for Br) implemented in Gaussian 09 suite of programs.[56] Stationary structures are obtained by confirming that all the harmonic frequencies are real. Structures of the transition states are obtained by observing only one imaginary harmonic frequency, and also by carrying out the intrinsic reaction coordinate analysis along the reaction pathway. Zero point energies (ZPEs) are taken into account. Default criteria are used for all optimizations. To reduce computational efforts, we adopt C_3H_7OMs as the model substrate for 2-(3-methanesulfonyloxypropoxy) naphthalene, after finding that the naphthalene ring and the ether group do not play any significant role in the S_N2 reactions studied here. Relative Gibbs energies (at 90 °C) of pre-reaction complexes were calculated to compare their thermodynamic stability, and activation barriers $G^{\ddagger}$ of alternative reaction paths were evaluated to determine the most feasible reaction pathway. In order to isolate the role of dihexaEGim we first interrogate the reaction mechanism in the absence of solvent.

2.2.1. Pre-reaction complexes. In Fig. 2 we present the lowest energy structures of pre-reaction complexes to see how the functional groups in dihexaEGIL interact with KX (X=F, Cl, Br) and the substrate. Several general features are to be noted: First, the counter-cation K^+ and the nucleophile X^- are far apart from each other with the distance of 4.3~6.6 Å in all pre-reaction complexes. Because the bond lengths[57] of gas phase KF, KCl, and KBr are 2.171, 2.667, 2.821 Å, respectively, this indicates that the metal salt KX is essentially separated to form a 'naked' nucleophile that is almost free from the Coulombic influence of the counter-cation K^+. The six O atoms of a hexaEG moiety coordinate K^+, whereas the other hexaEG interacts with the imidazolium cation, with a hydroxyl O



Scheme 1. S_N2 reactions using KX (X=F, Cl, Br) promoted by [di-hexaEGim][OMs] in *tert*-amyl alcohol.

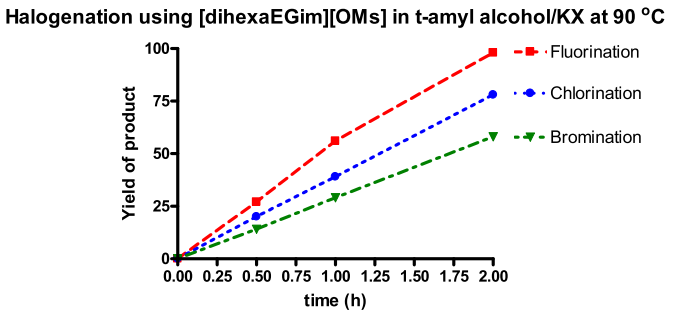


Fig. 1. Relative rates of S_N2 reactions of KX (X=F, Cl, Br) promoted by [dihexaEGmim][OMs] in *t*-amyl alcohol.

atom binding to the acidic 2-H. Second, the two −OH group, each from the two hexaEGs, act as 'anchor' to the nucleophile X^- in a configuration such that the backside attack of X^- on the substrate is most favorable. Third, the ionic liquid anion $[OMs]^-$ lying between the imidazolium and K^+ helps to mitigate the positive charge of K^+. The acidic 2-H in imidazolium is surrounded by the O atoms of hexaEG not interacting with K^+. Overall, the electronegative oxygen atoms, the acidic −OH, the imidazolium cation, $[OMs]^-$ anion, K^+, X^-, and the leaving group OMs^- in the substrate exert very intricate interactions with one another in a compact configuration that is extremely favorable for S_N2 reaction.

The three pre-reaction complexes for fluorination depicted in Fig. 2a mostly differ from each other in the orientation of the substrate chain relative to other parts of the complexes. The Gibbs

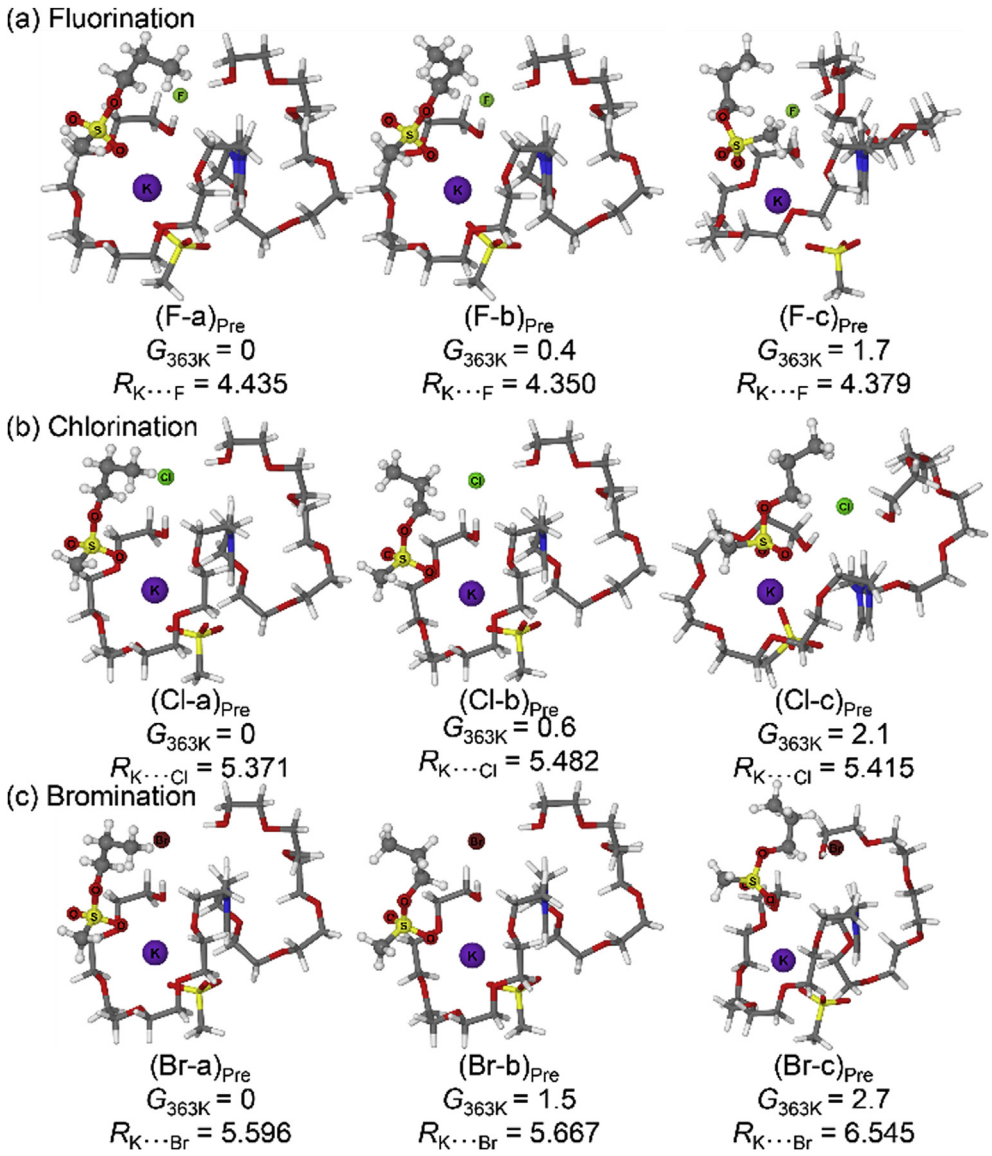


Fig. 2. Structures, relative Gibbs free energies (kcal/mol) at 90 °C and K … X (X=F, Cl, Br) distances (Å) of pre-reaction complexes with K^+ and X^- separated.

free energies at 90 °C of $(F\text{-}b)_{Pre}$ and $(F\text{-}c)_{Pre}$ are higher than $(F\text{-}a)_{Pre}$ by 0.4 and 1.7 kcal mol^{-1}, respectively. In the global minimum energy pre-reaction complexe $(F\text{-}a)_{Pre}$, the average distance $\tilde{R}_{K\ldots O}$ between K^+ and the coordinating O atoms of hexaEG, between K^+ and the two O atoms in $[OMs]^-$, between K^+ and the O atoms in leaving group are 3.053, 2.895 and 2.832 Å, respectively. The counter-cation K^+ is coordinated by nine O atoms in all. The nucleophile F^- forms hydrogen bonding with the two −OH groups of a dihexaEG with the distances of 1.469 and 1.476 Å. The two O atoms of OH groups of the other hexaEG are close to the 2-H in imidazolium with the distances of 2.532 and 1.957 Å. The metal salt KF is in separated form with $R_{K\ldots F}$=4.435 Å.

Since the energy of $(F\text{-}b)_{pre}$ is slightly higher (by 0.42 kcal mol^{-1}) than $(F\text{-}a)_{pre}$, this complex is almost as feasible as $(F\text{-}a)_{pre}$ in thermodynamic sense. The alkyl chain of the substrate in $(F\text{-}b)_{pre}$ is oriented in opposite direction to $(F\text{-}a)_{pre}$ (C−C−C−O torsional angles in $(F\text{-}a)_{Pre}$ and $(F\text{-}b)_{Pre}$ are 68.5° and −62.5°, respectively). The average distance $\tilde{R}_{K\ldots O}$ (3.053 Å) defined above is identical to that in $(F\text{-}a)_{Pre}$, and the distances (2.768, 3.018 Å) between K^+ and the two O atoms of $[OMs]^-$ are also similar to those in $(F\text{-}a)_{Pre}$. The nucleophile F^- interacts with the two −OH groups with the distances of 1.466 and 1.462 Å. The structure of $(F\text{-}c)_{Pre}$ is different from $(F\text{-}a)_{Pre}$ in two respects. First, only one O atom of $[OMs]^-$ coordinates to K^+ with shorter $R_{K\ldots O}$ of 2.700 Å. The other two O atoms are closer (2.336, 2.065 Å) to 4-C and 5-H. Second, the torsional angle of N−C bond between the imidazolium and hexaEG moieties is 96.2°, whereas those in $(F\text{-}a)_{Pre}$ and $(F\text{-}b)_{Pre}$ are −166.3, -166.2°, respectively. This large change in the torsional angle of N−C bond in $(F\text{-}c)_{Pre}$ from $(F\text{-}a)_{Pre}$ and $(F\text{-}b)_{Pre}$ seems to be the results of significant structural changes in hexaEG chain that is not binding to K^+ due to the thermodynamic stability obtained by the hydrogen bonding with F^- and interactions between −OH and imidazolium 2-H.

The structures of $(Cl\text{-}a)_{Pre}$ and $(Cl\text{-}b)_{Pre}$ are similar to those of $(F\text{-}a)_{Pre}$ and $(F\text{-}b)_{Pre}$. The lengths of hydrogen bonding in $(Cl\text{-}a)_{Pre}$ ($(Cl\text{-}b)_{Pre}$) between −OH in di-hexaEG and Cl^- are 2.080, 2.096 Å (2.080, 2.082 Å), and $\tilde{R}_{K\ldots O}$=3.023 Å (3.002 Å). The most conspicuous structural difference between the $(Cl\text{-}a)_{Pre}$ and $(Cl\text{-}b)_{Pre}$ is the C−C−C−O torsional angle (64.9, −64.0° for $(Cl\text{-}a)_{Pre}$ and $(Cl\text{-}b)_{Pre}$, respectively), resulting from the different orientations of the alkyl chain. On the other hand, the structure of $(Cl\text{-}c)_{Pre}$ is somewhat distinct in that Cl^- interacts both with −OH of dihexaEG and

imidazolium 2-H. The distance ($R_{Cl \cdots 2\text{-}H}$=2.424 Å) of the latter is considerably shorter than those (3.410, 3.455 Å) in (Cl-a)$_{Pre}$ and (Cl-b)$_{Pre}$. The three hydrogen bonds around Cl^- are expected to decrease the nucleophilicity of Cl^- with larger activation barrier. The other structural features around K^+ in (Cl-c)$_{Pre}$ (K^+ coordinated by six hexaEG O atoms ($\tilde{R}_{K \cdots O}$=3.000 Å), by two O atoms of $[OMs]^-$ ($R_{K \cdots O}$=2.860, 2.927 Å), and a O atom of the leaving group C_3H_7OMs ($R_{K \cdots O}$=2.908 Å) are similar to (Cl-a)$_{Pre}$ and (Cl-b)$_{Pre}$.

The structures of pre-reaction complexes in S_N2 bromination (Fig. 2c) are similar to those described for fluorination with the exception of (Br-c)$_{Pre}$. In the global minimum energy pre-reaction complex (Br-a)$_{Pre}$, $\tilde{R}_{K \cdots O}$ is 3.018 Å, the distance between the counter-cation K^+ and leaving group is 2.842 Å, and that between K^+ and the two O atoms of $[OMs]^-$ are 2.793, 2.934 Å. The two hydroxyl −OH bind to the nucleophile Br^- with $R_{Br \cdots OH}$=2.300, 2.319 Å. In the complex (Br-b)$_{Pre}$, whose G_{363K} is 1.48 kcal mol^{-1} higher than (Br-a)$_{Pre}$, the C−C−C−O torsional angle (−64.1°) is similar to that (−62.5°) in (F-b)$_{Pre}$. $\tilde{R}_{K \cdots O}$ is 3.112 Å, the distance between K^+ and the two O atoms in $[OMs]^-$ are 2.819, 2.946 Å, and those between the two hydroxyl −OH and Br^- are 2.294, 2.304 Å. In contrast with these two lower energy complexes, the acidic 2-H in (Br-c)$_{Pre}$ interacts with Br^- ($R_{Br \cdots O}$=2.572 Å) rather than with the hydroxyl O atoms of hexaEG. The torsional angle of the N−C bond between the imidazolium and hexaEG far from K^+ is −138.8°, very different from those (∼160°) in other pre-reaction complexes. Also, the −OH groups in hexaEG lying far from K^+ bend toward the O atoms of the leaving group, rather than toward Br^-. The leaving group −OMs in (Br-c)$_{Pre}$ does not coordinate to K^+, and the total number (8) of O atoms binding to K^+ is smaller than in other complexes. These structural features results in G_{363K} of this complex somewhat (by 2.7 kcal mol^{-1}) higher than (Br-a)$_{Pre}$.

In comparison with these pre-reaction complexes with the separated nucleophile and counter-cation, Fig. 3 presents the corresponding pre-reaction complexes with KX (X=F, Cl, Br) in the form of contact ion-pair (CIP). It can be seen that the $R_{K \cdots X}$ distances (2.710, 3.314 and 3.553 Å for X=F, Cl, Br) in these complexes are a bit larger than those (2.171, 2.667, 2.821 Å) in the gas phase ion pair due to the interactions with the promotor, but still far smaller than those shown in Fig. 2. The G_{363K} (5.0∼5.9 kcal mol^{-1}) of these complexes relative to (F-a)$_{Pre}$, (Cl-a)$_{pre}$ and (Br-a)$_{Pre}$ indicate that the population of these pre-reaction complexes with shorter $R_{K \cdots X}$ distances would be very small (<0.01%) compared with the more stable complexes (F-a)$_{Pre}$, (Cl-a)$_{pre}$ and in (Br-a)$_{Pre}$ given in Fig. 2. This manifested thermodynamic stability of pre-reaction complexes with separated K … X relative to those with KX CIP strongly indicates that the promotor dihexaEGIL dissociates the metal salts almost completely, due to the coordination by the O atoms in the promotor on K^+ that is more than enough to overcome the strong Coulombic forces between K^+ and the nucleophile. Considering that cryptands such as crown ethers may not easily separate the metal cation from the anion,[43–47] and that even water may not completely dissociate the metal salts (e.g., 20∼30% of LiCl is still in contact ion pair form ($R_{Li \cdots Cl}$=2.1 Å) in 1.3 (M) aqueous solution),[51] we believe that our observation is a significant advance in ion-pair chemistry.[48–52]

2.2.2. Reaction mechanism. Fig. 4 illustrates the transition states and energy profiles of the most feasible reaction pathways of S_N2

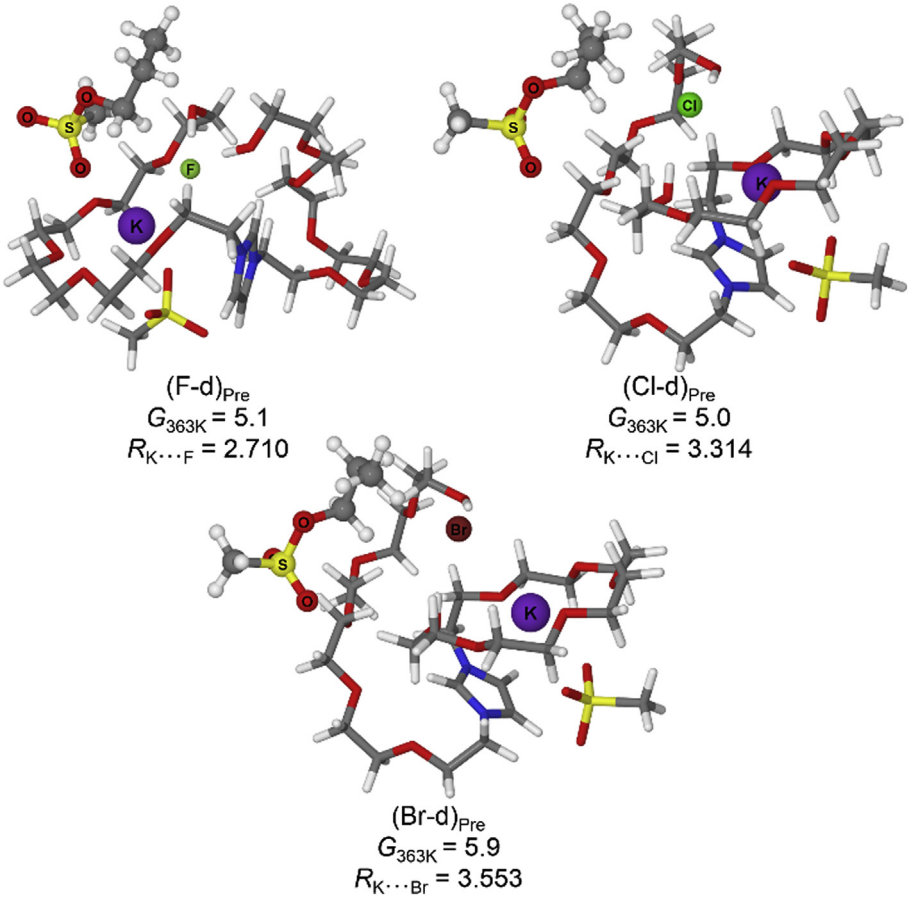


Fig. 3. Structures, relative Gibbs free energies (Kcal mol^{-1}) at 90 °C and K … X (X=F, Cl, Br) distances (Å) of pre-reaction complexes in which the nucleophile and the counter-cation are in the form of ion-pair.

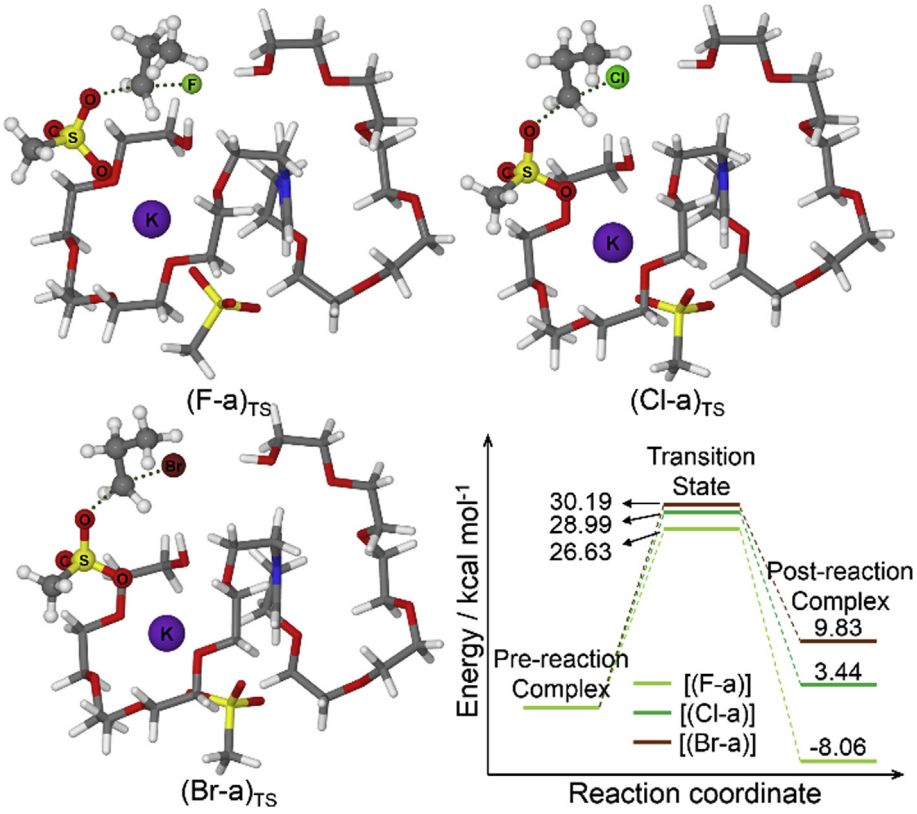


Fig. 4. Structures of transition states and energy profile of S_N2 reaction pathways in the absenc of solvent.

reactions, including the Gibbs free energy of activation $G^{\ddagger}_{363K}$. We find that all S_N2 reactions proceed from the lowest energy pre-reaction complexes $(F\text{-}a)_{Pre}$, $(Cl\text{-}a)_{Pre}$, and $(Br\text{-}a)_{Pre}$ given in Fig. 2. The distances $\tilde{R}_{K\ldots O}$, $R_{K\ldots OMs}$, $R_{K\ldots [OMs]}$ in $(F\text{-}a)_{TS}$ slightly decrease to 3.024, 2.769, 2.704 Å, respectively, as compared with the pre-reaction complex $(F\text{-}a)_{Pre}$, and K^+ is now coordinated by an O atom of $[OMs]^-$ in $(F\text{-}a)_{TS}$ rather than by two O atoms. The counter-cation K^+ is thus coordinated by eight O atoms, with one of the two O atoms of $[OMs]^-$ being moved away from K^+ to $R_{K\ldots O}$=3.811 Å. The −OH groups of dihexaEG moiety, on the other hand, are closer to F^- (1.592, 1.601 Å), and the counter-cation is separated from the nucleophile farther in the transition state to $R_{K\ldots F}$=4.645 Å. The distances between F^- and the reaction center C is 1.893 Å, and ∠F−C−O=167.9°. In the transition state $(Cl\text{-}a)_{TS}$ for chlorination, $R_{Cl\ldots OH}$ increases to 2.209 Å from 2.080 Å in $(Cl\text{-}a)_{Pre}$, $R_{K\ldots OMs}$ decreases to 2.749 Å from 2.843 Å, and K^+ is coordinated by eight O atoms, as also observed for fluorination. In contrast with $(F\text{-}a)_{TS}$ and $(Cl\text{-}a)_{TS}$, on the other hand, the counter-cation K^+ in the transition state for bromination $(Br\text{-}a)_{TS}$ interacts with nine O atoms: six O atoms of hexaEG ($\tilde{R}_{K\ldots O}$=3.023 Å), an O atom of the leaving group ($R_{K\ldots O}$=2.739 Å), and two O atoms of the anion $[OMs]^-$ ($R_{K\ldots O}$=2.790, 3.086 Å).

The calculated $G^{\ddagger}_{363K}$ for fluorination, chlorination and bromination are 26.6, 29.0, and 30.2 kcal mol^{-1}, respectively, indicating that the rates of reaction are in the order $F^->Cl^->Br^-$ in good agreement with the experimental observations in Fig. 1. The calculated differences in activation barriers seem, however, to be somewhat larger than experimentally observed relative S_N2 rates, presumably because the calculated gas phase (i.e., in the absence of solvent) free energies of activation $G^{\ddagger}_{363K}$ for S_N2 reactions may not account for differences in solubility of metal salts KF, KCl and KBr that may have affected the experimental rates of reactions. If these metal salts are equally soluble in solvent, the differences in $G^{\ddagger}_{363K}$ would be more equivalent to the observed differences in rate constants. Because the solubility KF in *tert*-amyl alcohol is smaller than those of KCl and KBr, this smaller effective concentration of KF seems to give lower relative rate for fluorination than that predicted by the calculated differences in $G^{\ddagger}_{363K}$.

2.3. Role of the solvent *t*-amyl alcohol

The influence of solvent *tert*-amyl alcohol is also of considerable interest, because S_N2 reactions were previously observed to be promoted by bulky alcohols alone, which acts as Lewis base on the counter-cation.[24–26] Fig. 5 presents the structures of pre-reaction complexes for S_N2 reactions in the presence of a *tert*-amyl alcohol molecule. We find that the *tert*-amyl alcohol molecule may either interact with the nucleophile X^- or with the ionic liquid anion $[OMs]^-$. In the former case ($(F\text{-}a\text{-}1)_{Pre}$, $(Cl\text{-}a\text{-}1)_{Pre}$, $(Br\text{-}a\text{-}1)_{Pre}$), the *tert*-amyl alcohol molecule acts as a Lewis acid on X^-, exerting a direct and retarding effect on the nucleophilicity of X^-. In the latter situation ($(F\text{-}a\text{-}2)_{Pre}$, $(Cl\text{-}a\text{-}2a)_{Pre}$, $(Cl\text{-}a\text{-}2b)_{Pre}$, $(Br\text{-}a\text{-}2)_{Pre}$), the solvent molecule interacts with $[OMs]^-$ as a hydrogen bond donor, affecting the S_N2 rates indirectly. The thermodynamic stabilities of these two types of pre-reaction complexes are quite similar, the differences being only 0.3–1.2 kcal mol^{-1}. Therefore, the relative feasibility of the reactions proceeding from each type of pre-reaction complexes would mostly be determined by the magnitudes of the activation barriers of the two reaction pathways from these two types of pre-reaction complexes.

In the global minimum energy structure $(F\text{-}a\text{-}1)_{Pre}$ for fluorination, the *tert*-amyl alcohol acts as a hydrogen bond donor to F^-, which forms three hydrogen bonds also with the two −OH groups of dihexaEG. The torsional angle (C−C−C−O) (−64.0°) designating the orientation of the alkyl chain in the substrate (C_3H_7OMs) is similar to that (−62.5°) in $(F\text{-}b)_{Pre}$., and the counter-cation K^+ is also

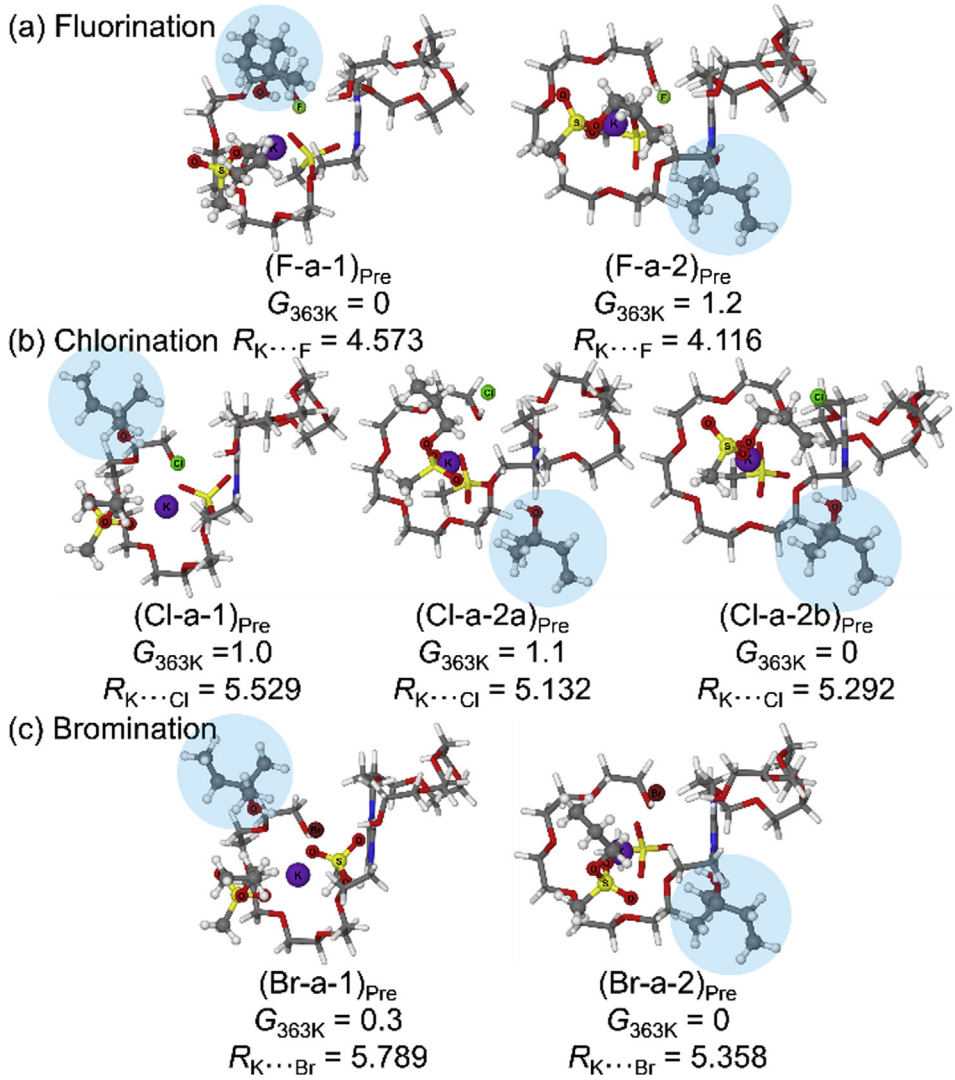


Fig. 5. Structures of pre-reaction complexes under the influence of a solvent (*tert*-amyl alcohol in circle) molecule (Relative G_{363K} in kcal mol^{-1}).

coordinated by nine O atoms. As the reaction proceeds, the distance between F^- and *tert*-amyl alcohol increases 1.642→1.720→2.010 Å.

In $(F\text{-a-}2)_{Pre}$ the *tert*-amyl alcohol molecule forms a hydrogen bond with the ionic liquid anion $[OMs]^-$, far from either F^- or K^+. Only one of the O atoms of $[OMs]^-$ coordinates to K^+, $R_{K\ \cdots\ [OMs]^-}$=2.686 Å. The −OH of *tert*-amyl alcohol is close to the −OH of $[OMs]^-$ with the distance 1.790 Å. In contrast to the pre-reaction complex in the absence of a solvent molecules, in which the O atom of $[OMs]^-$ is very close to the imidazolium 4 and 5-H, the solvent−OH in $(F\text{-a-}2)_{Pre}$ acting as a hydrogen bond acceptor to the imidazolium also plays a role of a hydrogen bond donor to $[OMs]^-$. The lengths (1.469, 1.476 Å) of hydrogen bonding between F^- and dihexaEG are similar to those in the absence of solvent molecule, because the *tert*-amyl alcohol molecule is far from the reaction center.

Fig. 5 (b) depicts the three lowest energy pre-reaction complexes for S_N2 chlorination. As in $(Cl\text{-a})_{Pre}$, both dihexaEG −OH and *tert*-amyl alcohol in $(Cl\text{-a-}1)_{Pre}$ interact with Cl^- by hydrogen bonding. The position of *tert*-amyl alcohol in this structure is similar to that in $(F\text{-a-}1)_{Pre}$. Both in $(Cl\text{-a-}2a)_{Pre}$ and $(Cl\text{-a-}2b)_{Pre}$, the *tert*-amyl alcohol molecule binds to $[OMs]^-$, Cl^- forms hydrogen bonding with dihexaEG −OH, and K^+ is coordinated by six O atoms from hexaEG and two O atoms from $[OMs]^-$. The positions of Cl^- are, however, very different from each other: While the imidazolium 2-H in $(Cl\text{-a-}2a)_{Pre}$ interacts with the O atom of hexaEG and the −OH acts as a Lewis acid on Cl^- in the form of $2\text{-}H_{(Imidazolium)}\ -OH_{(hexaEG)}\ \cdots\ Cl^-$, Cl^- binds directly to imidazolium in $(Cl\text{-a-}2b)_{Pre}$ ($R_{2\text{-}H(Imidazolium)\ \cdots\ Cl}$=2.603 Å). In $(Br\text{-a-}1)_{Pre}$ the *tert*-amyl alcohol molecule and Br^- interact, directly affecting the S_N2 bromination. The nucleophile Br^- forms three hydrogen bonds with *tert*-amyl alcohol ($R_{Br\ \cdots\ OH}$=2.446 Å), and with the two dihexaEG −OH, with the distances (2.322, 2.376 Å) of the latter interactions being slightly larger than those (2.300, 2.319 Å) in the absence of solvent molecule. During the reaction the distance between K^+ and the leaving group (between Br^- and *tert*-amyl alcohol −OH) decreases (increases) 2.836→2.776→2.768 Å (2.446→2.548→2.877 Å).

Figs. 6 and 7 depict the structures of transition stats for S_N2 reactions under the influence of solvent (*tert*-amyl alcohol), and Table 1 summarizes the energetics of S_N2 reaction pathways. The Gibbs free energies of activation $G^{\ddagger}_{363K}$ for reactions from $(F\text{-a-}1)_{Pre}$, $(Cl\text{-a-}1)_{Pre}$, and $(Br\text{-a-}1)_{Pre}$ are 29.3, 31.8, and 32.4 kcal mol^{-1}, respectively. Although the trend ($F^-<Cl^-<Br^-$) in $G^{\ddagger}_{363K}$ is consistent with experimental observations of relative rates ($F^->Cl^->Br^-$) of S_N2 reactions via the first type transition states ($(F\text{-a-}1)_{TS}$, $(Cl\text{-a-}1)_{TS}$, $(Br\text{-a-}1)_{TS}$; Fig. 6), the barriers are larger (by 2.2–2.7 kcal mol^{-1}) than those calculated in the absence of solvent. In contrast, the S_N2 pathways via the second type transition states

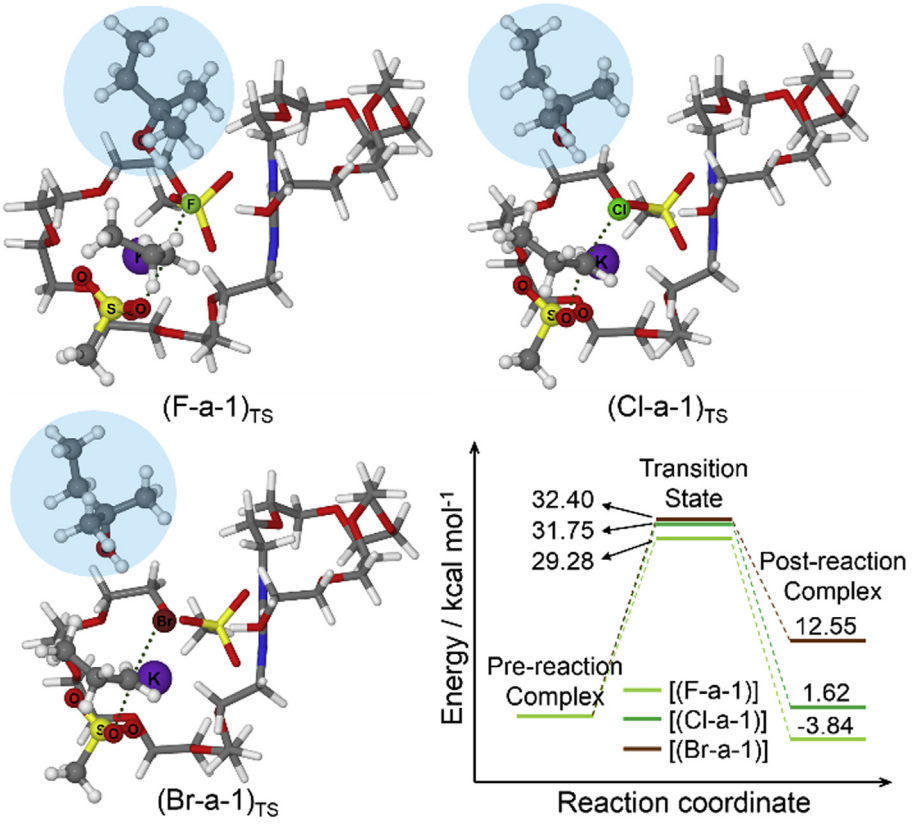


Fig. 6. Structures of transition states and energy profiles of S_N2 reaction pathways proceeding from the pre-reaction complexes ($(F\text{-}a\text{-}1)_{Pre}$, $(Cl\text{-}a\text{-}1)_{Pre}$, and $(Br\text{-}a\text{-}1)_{Pre}$) under the influence of solvent (*tert*-amyl alcohol in circle) molecule interacting with the nucleophile X^-. Effective barriers (relative energy from the global minimum energy structure plus teh activation barrier) in kcal mol^{-1}.

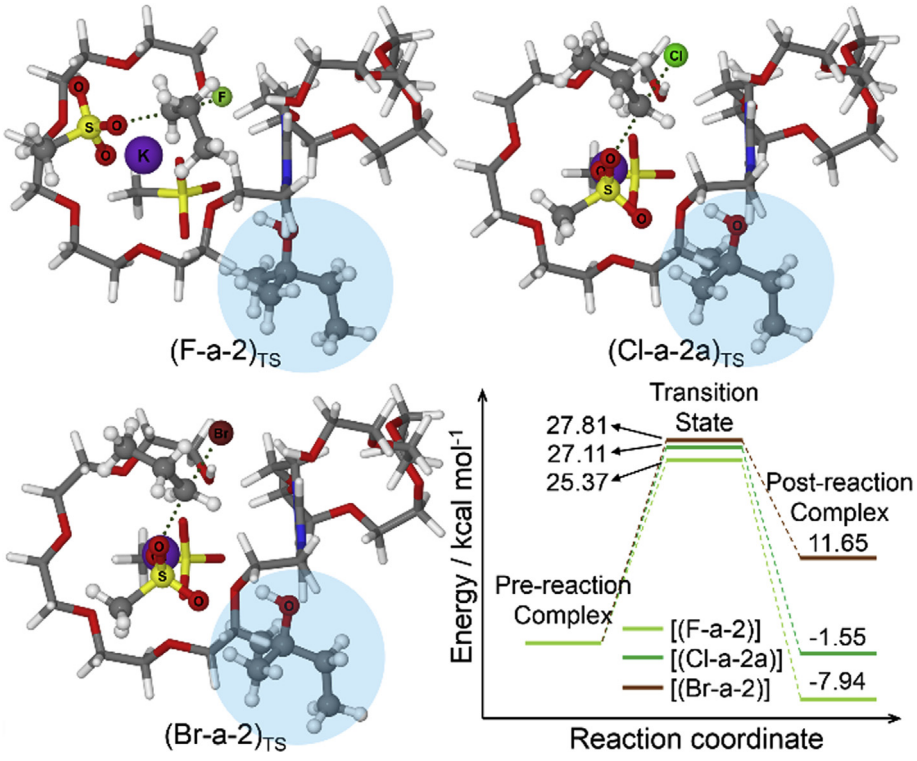


Fig. 7. Structures of transition states and energy profiles of S_N2 reaction pathways proceeding from the pre-reaction complexes ($(F\text{-}a\text{-}2)_{Pre}$, $(Cl\text{-}a\text{-}2a)_{Pre}$, and $(Br\text{-}a\text{-}2)_{Pre}$) under the influence of solvent (*tert*-amyl alcohol) molecule interacting with the anion $[OMs]^-$.

Table 1
Energetics (in kcal mol^{-1}) of S_N2 reaction pathways under the influence of a *tert*-amyl alcohol molecule

Pathway	$G^{\ddagger}_{363K}$	ΔG_{363K}[a]	G_{363K}[b]	Effective barrier	Solvent position	
(F-a-1)	29.28	−3.84	0	29.28	Direct	Global minimum pathway
(Cl-a-1)	30.72-	0.58	1.04	31.75		
(Br-a-1)	32.07	12.23	0.32	32.40		
(F-a-2)	24.15	−9.16	1.22	25.37	Indirect	Lowest effective barrier
(Cl-a-2a)	25.98	−0.16	1.14	27.11		Lowest effective barrier
(Cl-a-2b)	28.83	−1.55	0	28.83		Global minimum pathway
(Br-a-1)	27.81	11.65	0	27.81		Global minimum pathway

[a] Free energy of reaction ΔG363K.
[b] Relative G363K of pre-reaction complexes.

($(F\text{-}a\text{-}2)_{TS}$, $(Cl\text{-}a\text{-}2)_{TS}$, $(Br\text{-}a\text{-}2)_{TS}$; Fig. 7), in which the solvent molecule binds to the ionic liquid anion $[OMs]^-$, exhibit the net barriers (25.4, 27.1, 27.8 kcal mol^{-1} for F^-, Cl^-, Br^-, respectively) that are *lower* (by 1.2∼2.4 kcal mol^{-1}) than the solvent-free $G^{\ddagger}_{363K}$. The trend ($F^-<Cl^-<Br^-$) of the net barriers is also in line with the experimental observations of relative S_N2 reactivity (fluorination>chlorination>bromination). This indicates that the solvent molecule may considerably promote the S_N2 reactions, although it lies pretty far from the nucleophile or the counter-cation. The origin of the latter effects may be understood by the interactions of the *tert*-amyl alcohol molecule with $[OMs]^-$: The solvent molecule binds to the O atoms of $[OMs]^-$ as a hydrogen bond donor (Lewis acid), offsetting their partial negative charges. This in turn may weaken the interactions between the O atoms of $[OMs]^-$ and K^+, allowing the counter-cation to attract the O atoms of hexaEG and the leaving group C_3H_7OMs more strongly. The values of $R_{K\ldots OMs}$ ($\tilde{R}_{K\ldots O}$) in the transition states $(X\text{-}a)_{TS}$ (X=F, Cl, Br) of S_N2 reactions in the absence of solvent significantly decrease when a *tert*-amyl alcohol molecule influences the reactions in $(X\text{-}a\text{-}2)_{TS}$: For X=F, 2.769 (3.024)→2.754 (3.012) Å, For X=Cl, 2.749 (3.027)→2.740 (3.001) Å, and for X=Br, 2.739 (3.023)→2.731 (3.010 Å).

The net effects of these interactions seem to give lower activation barriers when the reaction occurs under the influence of a *tert*-amyl alcohol molecule than those in the absence of solvent. Although the Gibbs free energy of $(F\text{-}a\text{-}1)_{Pre}$ is slightly lower (by 1.22 kcal mol^{-1}), the Gibbs energy of activation ($G^{\ddagger}_{363K}$=25.4 kcal mol^{-1}) for fluorination reaction proceeding from the pre-reaction complex $(F\text{-}a\text{-}2)_{Pre}$ is significantly (by 3.9 kcal mol^{-1}) lower than the reaction pathway starting from $(F\text{-}a\text{-}1)_{Pre}$. Therefore, the S_N2 fluorination reaction may be considered to proceed via the transition state $(F\text{-}a\text{-}2)_{TS}$, because the net barrier (26.6 kcal mol^{-1}) from $(F\text{-}a\text{-}2)_{Pre}$ obtained by adding the difference (1.22 kcal mol^{-1}) in G_{363K} between $(F\text{-}a\text{-}1)_{Pre}$ and $(F\text{-}a\text{-}2)_{Pre}$ to the activation barrier (25.4 kcal mol^{-1}) $G^{\ddagger}_{363K}$ from $(F\text{-}a\text{-}2)_{Pre}$ is lower. Similarly, the most feasible pathway of S_N2 chlorination reaction would occur from (Cl-a-2a), because net activation barrier (27.1 kcal mol^{-1}) from (Cl-a-2a) is slightly (by 1.1 kcal mol^{-1}) is lower than that (28.8 kcal mol^{-1}) from $(Cl\text{-}a\text{-}2b)_{Pre}$. The reaction pathway for S_N2 bromination reaction would be determined by comparing the activation barriers from the $(Br\text{-}a\text{-}1)_{Pre}$ and $(Br\text{-}a\text{-}2)_{Pre}$, because the thermodynamic stabilities of the two pre-reaction complexes are almost equal (the difference in $G^{\ddagger}_{363K}$ is only 0.3 kcal mol^{-1}). Bromination pathway via the transition state $(Br\text{-}a\text{-}2)_{TS}$ with lower activation barrier (27.8 kcal mol^{-1}) is clearly more preferable.

3. Conclusion

Our present theoretical study clearly demonstrates that the experimentally observed excellent efficiency of dihexaEGim for accelerating the S_N2 halogenation reactions stems mainly from the role of the promotor separating the metal halides and thus producing the 'naked' nucleophiles. The low rate of S_N2 fluorination relative to those of chlorination and bromination usually observed in polar organic solvents is reversed here, demonstrating the influence of the promotor. The solvent *tert*-amyl alcohol is found to play an indirect role in the present system, in contrast to our previous study of S_N2 reactions that were directly promoted by bulky alcohols and oligoethylene glycols. The order of nucleophilicity of F^-, Cl^- and Br^- is observed to be the same as the order of basicity $F^->Cl^->Br^-$, because the nucleophiles are essentially free from the influence of the counter-cation and solvent molecules. The usually observed side reactions such as E2 elimination for strongly basic nucleophiles such as F^- doesn't seem to be problematic here due to the very compact arrangement of the participants (nucleophile, counter-cation, promotor, solvent and the substrate) that is ideal configurations for the S_N2 attack by the nucleophile on the substrate in the pre-reaction complexes.

4. Experimental section

4.1. General

Unless otherwise noted, all reagents and solvents were commercially available. Reaction progress was followed by TLC on 0.25 mm silica gel 60 aluminium sheets containing F-254 indicator. Visualization on TLC was monitored by UV light. Flash chromatography was performed with 230–400 mesh silica gel. ^1H and ^{13}C NMR spectra were recorded on a 400 or 600 MHz spectrometer, and chemical shifts were reported in δ units (ppm) relative to tetramethylsilane. Low- and high-resolution electron impact (EI, 70 eV) spectra were obtained.

4.2. Analytical data of [dihexaEGim][OMs]

Prepared by using reported procedure[41]; ^1H NMR (600 MHz, $CDCl_3$) δ 2.78 (s, 3H), 3.58 (t, J=6.0 Hz, 4H), 3.60–3.71 (m, 36H), 3.89 (t, J=6.0 Hz, 4H), 4.52 (t, J=6.0 Hz, 4H), 7.58 (d, J=1.4 Hz, 2H), 9.69 (s, 1H); ^{13}C NMR (150 MHz, $CDCl_3$) δ 39.60, 49.67, 61.49, 69.30, 70.25, 70.31, 70.40, 70.47, 70.56, 70.64, 72.74, 122.98, 137.71; MS (FAB) m/z 597 (M^+–X, 100); HRMS (FAB) m/z calcd for $C_{27}H_{53}O_{12}N_2$ (M^+–X) 597.3599, found 597.3601; (X=[OMs]).

4.3. Procedure and analytical data of halogenations (Fig. 1)

4.3.1. Fluorination. KF (174 mg, 3 mmol) was added to the mixture of mesylate **1** (281 mg, 1.0 mmol), [hexaEGmim][OMs] (221 mg, 0.5 mmol), and *t*-amyl alcohol (4 mL) in a reaction vial. The reaction mixture was stirred for 2 h at 90 °C. The reaction time was determined by checking TLC. The reaction mixture was filtered and washed with diethyl ether, and the filtrate was evaporated under reduced pressure. Flash column chromatography (10% EtOAc/hexanes) of the filtrate afforded 201 mg (0.98 mmol, 98%) of 2-(3-fluoropropoxy)naphthalene (**2**) as a colorless oil. ^1H NMR (400 MHz, $CDCl_3$) δ 2.14–2.39 (m, 2H), 4.24 (t, J=6.2 Hz, 2H), 4.72 (dt, J=46.8, 5.8 Hz, 2H), 7.16–7.22 (m, 2H), 7.34–7.53 (m, 2H), 7.76–7.83 (m, 3H); ^{13}C NMR (100 MHz, $CDCl_3$) δ 30.4 (d, J=20.1 Hz), 63.6 (d, J=25.3 Hz), 80.8 (d, J=163.9 Hz), 106.8, 118.8, 123.6, 126.4, 126.7, 127.6, 129.1, 129.4, 134.6, 156.7; MS (EI) m/z 204 (M^+); HRMS (EI) m/z calcd for $C_{13}H_{13}FO(M^+)$ 204.0950, found 204.0932.[30]

4.3.2. Chlorination. The preparation followed the procedure of fluorination except that KCl (224 mg, 3.0 mmol) was used and stirred the reaction mixture at at 90 °C for 2 h to obtain 171 mg (0.78 mmol, 78%) of 2-(3-chloropropoxy)naphthalene (**3**) as a colorless oil: ^1H NMR (600 MHz, $CDCl_3$) δ 2.28–2.32 (m, 2H), 3.79 (t, J=6.2 Hz, 2H), 4.23 (t, J=6.2 Hz, 2H), 7.12–7.15 (m, 2H), 7.34 (t,

J=6.8 Hz, 1H), 7.44 (t, J=6.8 Hz, 1H), 7.72–7.77 (m, 3H); ^{13}C NMR (100 MHz, $CDCl_3$) δ 32.17, 41.60, 64.17, 106.56, 118.76, 123.65, 126.38, 126.71, 127.61, 128.94, 129.41, 134.44, 156.57; MS (EI) m/z 220 (M^+), 144, 115; HRMS (EI) m/z calcd for $C_{13}H_{13}OCl$ (M^+) 220.0655; found 220.0667.[30]

4.3.3. Bromination. The preparation followed the procedure of fluorination except that KBr (357 mg, 3.0 mmol) was used and stirred the reaction mixture at at 90 °C for 2 h to obtain 153 mg (0.58 mmol, 58%) of 2-(3-bromopropoxy)naphthalene (**4**) as a colorless oil: ^{1}H NMR (400 MHz, $CDCl_3$) δ 2.36–2.43 (m, 2H), 3.67 (t, J=6.6 Hz, 2H), 4.23 (t, J=5.6 Hz, 2H), 7.14–7.17 (m, 2H), 7.34–7.49 (m, 2H), 7.74–7.80 (m, 3H); ^{13}C NMR (100 MHz, $CDCl_3$) δ 30.1, 32.2, 65.2, 106.6, 118.8, 123.7, 126.4, 126.7, 127.6, 128.9, 129.4, 134.4, 156.5; MS (EI) m/z 264 (M^+), 266 (M^+), 144 (100), 115; HRMS (EI) m/z calcd for $C_{13}H_{13}O^{79}Br$ (M^+) 264.0150; found 264.0151.[30]

5. Analytical data of 2-(3-methanesulfonyloxypropoxy)naphthalene (1) as a starting material in Fig. 1

^{1}H NMR (200 MHz, $CDCl_3$) δ 2.24–2.36 (m, 2H), 3.00 (s, 3H), 4.22 (t, J=5.9 Hz, 2H), 4.50 (t, J=6.1 Hz, 2H), 7.10–7.15 (m, 2H), 7.31–7.49 (m, 2H), 7.71–7.79 (m, 3H); ^{13}C NMR (100 MHz, $CDCl_3$) δ 29.0, 37.1, 63.0, 66.8, 106.5, 118.6, 123.8, 126.4, 126.7, 127.6, 129.0, 129.5, 134.4, 156.3; MS (EI) m/z 280 (M^+, 100); HRMS (EI TOF) m/z calcd for $C_{14}H_{16}O_4S$ (M^+) 280.0769, found 280.0770.[30]

Acknowledgements

We thank the National Research Foundation of Korea (NRF-2012R1A2A2A02013289, NRF-2011-0021836, NRF-2014R1A2A2A03007401 and NRF-2014M2A2A7045045) for financial support and the KISTI Supercomputing Center (2014).

Supplementary data

Supplementary data related to this article can be found at http://dx.doi.org/10.1016/j.tet.2015.03.074.

References and notes

1. Smith, M. D.; March, J. *Advanced Organic Chemistry*, 5th ed.; Wiley and Sons: New York, NY, 2001; pp 389–674.
2. Makosza, M.; Wojciechowski, K. *Chem. Rev.* **2004**, *104*, 2631–2666.
3. Gerstenberger, M. R. C.; Haas, A. *Angew. Chem., Int. Ed. Engl.* **1981**, *20*, 647–667.
4. Müller, E.; Weyl, T.; Houben, J. In *Methoden Der Organischen Chemie*; Mueller, E., Ed.; Thieme: Stuttgart, Germany, 1962; Vol. 5/3.
5. Pliego, J. R., Jr.; Pilo-Veloso, D. *Phys. Chem. Chem. Phys.* **2008**, *10*, 1118–1124.
6. Pliego, J. R.; Piló-Veloso, D. *J. Phys. Chem. B* **2007**, *111*, 1752–1758.
7. Vayner, G.; Houk, K. N.; Jorgensen, W. L.; Brauman, J. I. *J. Am. Chem. Soc.* **2004**, *126*, 9054–9058.
8. Mo, S. J.; Vreven, T.; Mennucci, B.; Morokuma, K.; Tomasi, J. *Theor. Chem. Acc.* **2004**, *111*, 154–161.
9. Uggerud, E. *Chem.—Eur. J.* **2006**, *12*, 1127–1136.
10. Uggerud, E. *J. Phys. Org. Chem.* **2006**, *19*, 461–466.
11. Gonzales, J. M.; Cox, R. S.; Brown, S. T.; Allen, W. D.; Schaefer, H. F. *J. Phys. Chem. A* **2001**, *105*, 11327–11346.
12. Hernandez, M. I.; Campos-Martinez, J.; Villarreal, P.; Schmatz, S.; Clary, D. C. *Phys. Chem. Chem. Phys.* **1999**, *1*, 1197–1203.
13. Kim, S.-I.; Cho, H.-J.; Um, I.-H. *Bull. Korean Chem. Soc.* **2014**, *35*, 177–181.
14. O'Hair, R. A. J.; Davico, G. E.; Hacaloglu, J.; Dang, T. T.; DePuy, C. H.; Bierbaum, V. M. *J. Am. Chem. Soc.* **1994**, *116*, 3609–3610.
15. Craig, S. L.; Brauman, J. I. *J. Am. Chem. Soc.* **1999**, *121*, 6690–6699.
16. Jorgensen, W. L. *Acc. Chem. Res.* **1989**, *22*, 184–189.
17. Sun, L.; Song, K.; Hase, W. L. *Science* **2002**, *296*, 875–878.
18. Safi, B.; Choho, K.; Geerlings, P. *J. Phys. Chem. A* **2001**, *105*, 591–601.
19. Reichardt, C.; Welton, T. *Solvents and Solvent Effects in Organic Chemistry*, 4th ed.; Wiley-VCH: Weinheim, 2011.
20. Hutchins, R. O.; Taffer, I. M. *J. Org. Chem.* **1983**, *48*, 1360–1362.
21. Sowinski, A. F.; Whitesides, G. M. *J. Org. Chem.* **1979**, *44*, 2369–2376.
22. Kim, D. W.; Jeong, H. –J.; Lim, S. T.; Sohn, M.-H.; Katzenellenbogen, J. A.; Chi, D. Y. *J. Org. Chem.* **2008**, *73*, 957–962.
23. Kim, D. W.; Jeong, H. –J.; Lim, S. T.; Sohn, M.-H. *Angew. Chem., Int. Ed.* **2008**, *47*, 8404–8406.
24. Im, S.; Jang, S.-W.; Kim, H.-R.; Oh, Y.-H.; Park, S.-W.; Lee, S.; Chi, D. Y. *J. Phys. Chem. A* **2009**, *113*, 3685–3689.
25. Oh, Y.-H.; Ahn, D.-S.; Chung, S.-Y.; Jeon, J.-H.; Park, S.-W.; Oh, S. J.; Kim, D. W.; Kil, H. S.; Chi, D. Y.; Lee, S. *J. Phys. Chem. A* **2007**, *111*, 10152–10161.
26. Kim, D. W.; Ahn, D.-S.; Oh, Y.-H.; Lee, S.; Kil, H. S.; Oh, S. J.; Lee, S. J.; Kim, J. S.; Ryu, J. S.; Moon, D. H.; Chi, D. Y. *J. Am. Chem. Soc.* **2006**, *128*, 16394–16397.
27. Lee, J. W.; Yan, H.; Bin Jang, H.; Kim, H. K.; Park, S.-W.; Lee, S.; Chi, D. Y.; Song, C. E. *Angew. Chem., Int. Ed.* **2009**, *48*, 7683–7688.
28. Kim, D. W.; Chi, D. Y. *Angew. Chem., Int. Ed.* **2004**, *43*, 483–485.
29. Kim, D. W.; Song, C. E.; Chi, D. Y. *J. Org. Chem.* **2003**, *68*, 4281–4285.
30. Kim, D. W.; Song, C. E.; Chi, D. Y. *J. Am. Chem. Soc.* **2002**, *124*, 10278–10279.
31. Kim, J.-Y.; Kim, D. W.; Song, C. E.; Chi, D. Y.; Lee, S. *J. Phys. Org. Chem.* **2013**, *26*, 9–14.
32. Jadhav, V. H.; Jang, S. H.; Jeong, H.-J.; Lim, S. T.; Sohn, M.-H.; Kim, J.-Y.; Lee, S.; Lee, J. W.; Song, C. E.; Kim, D. W. *Chem. —Eur. J.* **2012**, *18*, 3918–3924.
33. Jadhav, V. H.; Jang, S. H.; Jeong, H.-J.; Lim, S. T.; Sohn, M.-H.; Chi, D. Y.; Kim, D. W. *Org. Lett.* **2010**, *12*, 3740–3743.
34. Oh, Y.-H.; Bin Jang, H.; Im, S.; Song, M. J.; Kim, S.-Y.; Park, S.-W.; Chi, D. Y.; Song, C. E.; Lee, S. *Org. Biomol. Chem.* **2011**, *9*, 418–422.
35. Welton, T. *Chem. Rev.* **1999**, *99*, 2071–2084.
36. Wasserscheid, P.; Keim, W. *Angew. Chem., Int. Ed.* **2000**, *39*, 3772–3789.
37. Tzschucke, C. C.; Markert, C.; Bannwarth, W.; Roller, S.; Hebel, A.; Haag, R. *Angew. Chem. Int. Ed.* **2002**, *41*, 3964–4000.
38. Zhao, H.; Malhotra, S. V. *Aldrichimica Acta* **2002**, *35*, 75–83.
39. Dupont, J.; Suarez, P. A. Z. *Phys. Chem. Chem. Phys.* **2006**, *8*, 2441–2452.
40. Tesfai, A.; El-Zahab, B.; Bwambok, D. K.; Baker, G. A.; Fakayode, S. O.; Lowry, M.; Warner, I. M. *Nano. Lett.* **2008**, *8*, 897–901.
41. Jadhav, V. H.; Jeong, H.-J.; Lim, S. T.; Sohn, M.-H.; Kim, D. W. *Org. Lett.* **2011**, *13*, 2502–2505.
42. Jadhav, V. H.; Kim, J.-Y.; Chi, D. Y.; Lee, S.; Kim, D. W. *Tetrahedron* **2014**, *70*, 533–542.
43. Müller, E.; Weyl, T.; Houben, J. *Methoden Der Organischen Chemie*; Thieme: Stuttgart, Germany, 1961, Vol. 5/4.
44. Gokel, G. W. *Crown Ethers and Cryptands*; Royal Society of Chemistry: Cambridge, UK, 1991.
45. Dehmlow, E. V.; Dehmlow, S. S. *Phase Transfer Catalysis*, 3rd ed.; VCH Ltd.: New York, NY, 1993.
46. Sun, H.; DiMagno, S. G. *J. Am. Chem. Soc.* **2005**, *127*, 2050–2051.
47. Pliego, J. R.; Riveros, J. M. *J. Mol. Catal. A: Chem.* **2012**, *363–364*, 489–494.
48. Sun, Z.; Zhang, W.; Ji, M.; Hartsock, R.; Gaffney, K. J. *J. Phys. Chem. B* **2013**, *117*, 15306–15312.
49. Finlayson-Pitts, B. J. *Chem. Rev.* **2003**, *103*, 4801–4822.
50. Marcus, Y.; Hefter, G. *Chem. Rev.* **2006**, *106*, 4585–4621.
51. Winkel, K.; Seidl, M.; Loerting, T.; Bove, L. E.; Imberti, S.; Molinero, V.; Bruni, F.; Mancinelli, R.; Ricci, M. A. *J. Chem. Phys.* **2011**, *134* 024515–024515.
52. Jungwirth, P. *J. Phys. Chem. B* **2014**, *118*, 10333–10334.
53. Lynch, B. J.; Fast, P. L.; Harris, M.; Truhlar, D. G. *J. Phys. Chem. A* **2000**, *104*, 4811–4815.
54. Adamo, C.; Barone, V. *J. Chem. Phys.* **1998**, *108*, 664–675.
55. Hay, P. J.; Wadt, W. R. *J. Chem. Phys.* **1985**, *82*, 299–310.
56. Frisch, M. J.; Trucks, G. W.; Schlegel, H. B.; Scuseria, G. E.; Robb, M. A.; Cheeseman, J. R.; Scalmani, G.; Barone, V.; Mennucci, B.; Petersson, G. A.; Nakatsuji, H.; Caricato, M.; Li, X.; Hratchian, H. P.; Izmaylov, A. F.; Bloino, J.; Zheng, G.; Sonnenberg, J. L.; Hada, M.; Ehara, M.; Toyota, K.; Fukuda, R.; Hasegawa, J.; Ishida, M.; Nakajima, T.; Honda, Y.; Kitao, O.; Nakai, H.; Vreven, T.; Montgomery, J. A., Jr.; Peralta, J. E.; Ogliaro, F.; Bearpark, M.; Heyd, J. J.; Brothers, E.; Kudin, K. N.; Staroverov, V. N.; Kobayashi, R.; Normand, J.; Raghavachari, K.; Rendell, A.; Burant, J. C.; Iyengar, S. S.; Tomasi, J.; Cossi, M.; Rega, N.; Millam, J. M.; Klene, M.; Knox, J. E.; Cross, J. B.; Bakken, V.; Adamo, C.; Jaramillo, J.; Gomperts, R.; Stratmann, R. E.; Yazyev, O.; Austin, A. J.; Cammi, R.; Pomelli, C.; Ochterski, J. W.; Martin, R. L.; Morokuma, K.; Zakrzewski, V. G.; Voth, G. A.; Salvador, P.; Dannenberg, J. J.; Dapprich, S.; Daniels, A. D.; Farkas, Ö.; Foresman, J. B.; Ortiz, J. V.; Cioslowski, J.; Fox, D. J. *Gaussian 09, Revision A.02*; Gaussian: Wallingford, CT, 2009.
57. Huber, K. P.; Herzberg, G. *Molecular Spectra and Molecular Structure IV: Constants of Diatomic Molecules*; Van Nostrand: New York, NY, 1979.